

International Journal of Modern Physics D
 © World Scientific Publishing Company

Gamma-Ray Burst Prompt Emission

BING ZHANG

Department of Physics and Astronomy, University of Nevada, Las Vegas, NV 89012, USA
zhang@physics.unlv.edu

Received Day Month Year

Revised Day Month Year

The origin of gamma-ray burst (GRB) prompt emission, bursts of γ -rays lasting from shorter than one second to thousands of seconds, remains not fully understood after more than 40 years of observations. The uncertainties lie in several open questions in the GRB physics, including jet composition, energy dissipation mechanism, particle acceleration mechanism, and radiation mechanism. Recent broad-band observations of prompt emission with Fermi sharpen the debates in these areas, which stimulated intense theoretical investigations invoking very different ideas. I will review these debates, and argue that the current data suggest the following picture: A quasi-thermal spectral component originating from the photosphere of the relativistic ejecta has been detected in some GRBs. Even though in some cases (e.g. GRB 090902B) this component dominates the spectrum, in most GRBs, this component either forms a sub-dominant “shoulder” spectral component in the low energy spectral regime of the more dominant “Band” component, or is not detectable at all. The main “Band” spectral component likely originates from the optically thin region due to synchrotron radiation. The diverse magnetization in the GRB central engine is likely the origin of the observed diverse prompt emission properties among bursts.

Keywords: Keyword1; keyword2; keyword3.

PACS numbers:

1. GRB prompt emission

Although discovered much earlier than the afterglow, the emission of gamma-ray bursts (GRBs) themselves, usually called the GRB *prompt emission*, is still poorly understood. The main uncertainties lie in several open questions in the GRB physics:¹

- What is the composition of the GRB jet?
- What is the energy dissipation mechanism in the jet?
- Where is the region of energy dissipation and prompt emission?
- What is the particle acceleration mechanism in the energy dissipation region?
- What is the radiation mechanism of the particles?

Among these, the answer to the first question is more fundamental, which decides or at least strongly affects the answers to the rest of the questions.

The traditional “fireball” model envisages a thermally-driven explosion, with gravitational energy released during a catastrophic event (such as massive star core collapse or merger of two compact stars) being deposited in the form of thermal heat at the base of the central engine. This fireball then expands under its own thermal pressure and gets accelerated to a relativistic speed, if baryon contamination in the ejecta is low enough.^{2,3} Most of the thermal energy is converted to the kinetic energy of the outflow,⁴ with some thermal energy released as photons at the photosphere.⁵ The kinetic energy of the outflow is further dissipated in the internal shocks⁶ and in the external (forward and reverse) shocks as the ejecta is decelerated by the ambient medium.^{7,8} The former powers the GRB prompt emission, while the latter powers the afterglow.^{9,10}

In contrast to the matter-dominated fireball picture, an opposite opinion is that the entire GRB phenomenology is electromagnetic. This is the electromagnetic (EM) model of GRBs.¹¹ Here the magnetic field plays the dominant role in ejecta dynamics. Little baryons are loaded from the central engine, so that an extremely high value of σ (ratio between Poynting flux and matter flux, or ratio between comoving magnetic energy density and rest mass energy density) is invoked. It is conjectured that σ remains extremely high ($\sim 10^5 - 10^6$) at the deceleration radius, so that the “sub-Alfvénic” condition $\sigma > \Gamma^2 - 1$ (Γ is the bulk Lorentz factor of the outflow) is satisfied. Within this scenario, the magnetic energy is directly converted to the particle energy and radiation energy through current instability around the deceleration radius. Such a scenario requires that the ejecta maintains high magnetization throughout, which is very difficult to achieve in reality.

More realistically, the GRB ejecta may carry both a matter component and a magnetic component. This results in a wide range of magnetohydrodynamic (MHD) models of GRBs.^{12–16} A real question is how high the σ parameter is. Since σ is a function of radius (magnetic acceleration and dissipation can constantly change σ in the flow), a more relevant question would be how high the σ parameter is at the GRB emission site. The complication is that one is not sure about the location of the GRB prompt emission radius R_{GRB} (see next section). The values of $\sigma(R_{\text{GRB}})$ and R_{GRB} are mutually dependent (and also depend on a third parameter, i.e. σ_0 at the central engine). Different GRB prompt emission models invoke different combinations of these parameters.

Observationally, the currently available information of GRB prompt emission includes the following aspects. A successful model should be able to interpret them.

- GRB lightcurves are extremely diverse.¹⁷ Some are spiky, while some others are smooth. Some have multiple (sometimes well separated) spiky episodes, while some others have one or two smooth pulses. Some are very long, while some others are very short. At least some lightcurves can be decomposed as the superposition of a fast and a slow component.¹⁸

- GRB spectra can be well characterized. For most GRBs, both the time-integrated and time-resolved spectra can be described by a so-called “Band” function, i.e. a smoothly-joint broken power law function characterized by three parameters: the low-energy and high-energy photon indices α and β , as well as the peak energy E_p in the energy spectrum.¹⁹ Recent Fermi LAT/GBM observations suggest that such a component dominates in nearly 7 orders of magnitude in energy in most GRBs.^{20,21} On the other hand, growing evidence suggests that this phenomenological function cannot fully account for the observations, and two additional spectral components, i.e. a quasi-thermal bump and a high-energy power-law component, are needed to fit the time-resolved data of bright GRBs.^{21–25}
- The peak energy E_p varies in a wide range, from as high as 15 MeV in GRB 110721A²⁴ to below 10 keV in GRB 060218.²⁶ It can evolve rapidly within a same burst, and two patterns can be identified: hard-to-soft evolution throughout a pulse or E_p intensity tracking.^{27,28}
- GRB polarization measurements have been made for some GRBs. Even though not with very high significance, evidence of high linear polarization degree for at least some bright GRBs has been collected.^{29,30}

The available data do not have “smoking gun” criteria to differentiate among the different models. Nonetheless, some available data already brought useful clues, serving as “finger prints” to diagnose the underlying physics of GRB prompt emission.

2. GRB prompt emission models

Before discussing the open questions and debates, it is informative to list various prompt emission models and their properties. In the following, we first categorize the models based on the location of GRB emission, i.e. the radius of emission from the central engine R_{GRB} . Swift observations of early X-ray afterglow suggest that the prompt emission site is “internal” (below the external shock where the jet is decelerated).³¹ The emission site is therefore bracketed between the photosphere radius R_{ph} (below which photons are opaque) and the deceleration radius R_{dec} (above which the jet decelerates due to jet-medium interaction). In the literature, several possible emission sites have been proposed. From small to large, they are, respectively,

- Photosphere radius R_{ph} : This radius is defined by the optically thin condition for electron Thomson scattering, i.e. the last scattering surface of photons originally trapped in the ejecta. The radius depends on luminosity L , Lorentz factor Γ , and the latitude with respect to the observer. For example, for a matter dominated outflow with photosphere radius above the coasting radius and for an on-axis observer, one has⁵ $R_{\text{ph}} \sim L\sigma_{\text{T}}/4\pi m_p c^3 \Gamma^3 \sim 3.7 \times 10^{11} \text{ cm } L_{52} \Gamma_{2.5}^{-3}$, where the convention

$Q_m = Q/10^m$ has been used. Considering angle-dependence of the optical depth, one gets a concave photosphere shape with respect to the line of sight.^{32,33}

- Internal shock radius R_{IS} : For a characteristic central engine variability time δt and Lorentz factor Γ , the internal shock radius can be estimated as⁶ $R_{\text{IS}} \sim \Gamma^2 c \delta t \sim 3 \times 10^{13} \text{ cm } \Gamma_{2.5}^2 \delta t_{-2}$. Since there is a range of δt in a GRB lightcurve, internal shocks can actually spread in a wide range of radii.
- Fast reconnection switch radius R_{rec} : If the outflow is magnetically dominated at small radii and the field configuration is *striped-wind-like*, McKinney & Uzdensky¹⁶ argued that a switch from the slow, collisional reconnection regime to the fast, collisionless reconnection regime occurs at around a radius $R_{\text{rec}} \sim 10^{13} - 10^{14} \text{ cm}$. The GRB emission is assumed to occur at this radius, which is above the photosphere.
- Internal-collision-induced magnetic reconnection and turbulence radius R_{ICMART} : If the outflow is magnetically dominated at small radii and the field configuration is *helical*, Zhang & Yan¹⁵ argued that rapid discharge of magnetic energy cannot be realized until the field lines are distorted enough through repetitive collisions. This radius is at least the internal shock radius (where collisions start), and should have a typical value $R_{\text{ICMART}} \sim 10^{15} - 10^{16} \text{ cm}$. Within this model, the slow variability component is related to the central engine activity, while the fast variability component is related to mini-jets due to relativistic turbulent reconnection,¹⁵ see also.^{11,34,35} So the emission radius may be estimated as $R_{\text{ICMART}} \sim \Gamma^2 c \delta T \sim 3 \times 10^{15} \text{ cm } \Gamma_{2.5}^2 \delta T$, where $\delta T \sim 1 \text{ s}$ is the variability time scale for the “slow” variability component.
- Deceleration radius R_{dec} : The deceleration radius R_{dec} is defined by the condition that the momentum collected from the ambient medium is comparable to the momentum in the jet. For a constant density medium, this is typically $R_{\text{dec}} \sim (3E/2\pi\Gamma^2 n m_p c^2)^{1/3} \sim 6.8 \times 10^{16} \text{ cm } E_{52}^{1/3} \Gamma_2^{-2/3} n^{-1/3}$. The electromagnetic model of GRBs¹¹ invokes current instabilities at this radius to power the observed GRBs. This is the largest radius allowed by the “internal” requirement of GRB prompt emission.

Keeping in mind of various emission radii, in the literature the following GRB prompt emission models have been discussed. The requirements for R_{GRB} and $\sigma(R_{\text{GRB}})$ for each model are summarized in Table 1.

- The fireball internal shock model:^{5,6,36,37} This is the standard theoretical framework. There are two emission sites in the model: the photosphere and the internal shocks. The magnetization parameter is $\sigma \ll 1$ in both locations.
- The magnetized engine - internal shock model: Some authors interpret the

observed GRB spectrum as synchrotron emission from the internal shocks only.^{38,39} An underlying assumption of such a model is that the photosphere emission is suppressed. This may appeal to a magnetized central engine.^{40,41} So the requirement of this model is $\sigma(R_{\text{ph}}) \gg 1$, and $\sigma(R_{\text{IS}}) \ll 1$. Some authors claim that it is possible that at the central engine $\sigma_0(R_0) \gg 1$, while at both the photosphere radius and internal shocks one has $\sigma(R_{\text{ph}}) \ll 1$, and $\sigma(R_{\text{IS}}) \ll 1$.⁴² Such a rapid magnetic acceleration has not been seen in numerical simulations.

- The dissipative photosphere model: Many authors^{14,43–52} argued that the observed GRB Band spectrum is simply the emission from the GRB photosphere. In order to reconcile the theoretically expected spectrum (quasi-thermal) and the data, one needs to introduce energy dissipation around the photosphere, probably due to internal shocks, proton-neutron collisions, or magnetic reconnections. Non-thermal electrons accelerated from the dissipative photosphere upscatter the seed thermal photons to make it non-thermal. The internal shock emission is neglected in this model. Several sub-categories of dissipative photosphere models have been discussed in the literature:
 - Collisional heating model:⁴⁷ Heating of photosphere is maintained via nuclear and/or Coulomb collisions. In this model, one has $\sigma(R_{\text{ph}}) \ll 1$ (to facilitate Coulomb collisions).
 - Magnetic dissipation model:^{14,51,52} Heating is maintained by magnetic reconnection near the photosphere. A striped-wind magnetic field configuration is required in order to facilitate rapid reconnection at such a small radius. To make efficient magnetic heating, one needs to have $\sigma(R_{\text{ph}}) \sim 1$. If $\sigma(R_{\text{ph}})$ is too high, the photosphere luminosity is suppressed by a factor $(1 + \sigma(R_{\text{ph}}))$.^{40,41,53} On the other hand, if $\sigma(R_{\text{ph}})$ is too low, the energy released via magnetic dissipation is small compared with the jet luminosity, so that the heating effect is not significant.
 - Jet-envelope interaction model:^{46,48,50} For long-duration GRBs that are believed to be associated with deaths of massive stars, a relativistic jet needs to penetrate through the stellar envelope first. The interaction between the jet and the stellar envelope inevitably introduces dissipation (through processes such as Kelvin-Helmholtz instabilities or collimation shocks). This dissipated energy can heat up the photosphere. In order to make such a mechanism effective, the photosphere cannot be too far away from the outer boundary of the stellar envelope. Otherwise photons would be quickly “thermalized” before reaching the photosphere.
- The internal collision-induced magnetic reconnection and turbulence (ICMART) model: This model¹⁵ invokes a large emission radius $R_{\text{ICMART}} \gg R_{\text{ph}}$. Once fast reconnection is triggered, the magnetic dissipation proceeds

6 *Zhang*

- in a run-away manner. The magnetization parameter $\sigma(R_{\text{ICMART}}) \geq 1$ when ICMART starts, and $\sigma(R_{\text{ICMART}}) \leq 1$ when ICMART is completed.
- The magnetic reconnection switch model: This model¹⁶ has $\sigma(R_{\text{rec}}) \geq 1$ to begin with, with σ continuously reducing with radius.
 - The current instability model: This model¹¹ invokes $\sigma(R_{\text{dec}}) \gg 1$. The σ value remains large beyond the dissipation radius.

Table 1. R_{GRB} and $\sigma(R_{\text{GRB}})$ for different models.

Model	R_{GRB}	$\sigma(R_{\text{GRB}})$	References
Fireball internal shock model	R_{ph} and R_{IS}	$\sigma(R_{\text{ph}}) \ll 1, \sigma(R_{\text{IS}}) \ll 1$	5, 6
Magnetized engine internal shock model	R_{IS}	$\sigma(R_{\text{ph}}) \gg 1, \sigma(R_{\text{IS}}) \ll 1$	38, 39
Collisional heating photosphere model	R_{ph}	$\sigma(R_{\text{ph}}) \ll 1$	47
Magnetic heating photosphere model	R_{ph}	$\sigma(R_{\text{ph}}) \lesssim 1$	14
ICMART model	R_{ICMART}	$\sigma_{\text{ICMART}} \geq 1 \rightarrow \leq 1$ ($\sigma(R_{\text{ph}}) \gg \sigma(R_{\text{IS}}) \gg 1$)	15
Reconnection switch model	R_{rec}	$\sigma(R_{\text{rec}}) \geq 1$	16
Current instability model	R_{dec}	$\sigma(R_{\text{dec}}) \gg 1$	11

3. Evolution of σ and Γ as a function of R .

To ease further discussion below, we first discuss how σ (and Γ) may evolve with radius R .

In general, a GRB jet launched from the central engine may have two components, one “hot” component due to neutrino heating from the accretion disk or the proto neutron star, and a “cold” component related to a magnetic Poynting flux launched from the black hole or the neutron star.^{54,55} The central engine can be characterized by a parameter

$$\mu_0 = \frac{L_w}{\dot{M}c^2} = \frac{L_h + L_c}{\dot{M}c^2} = \eta(1 + \sigma_0), \quad (1)$$

where $L_h = \eta\dot{M}$, $L_c = L_P$, and L_w are the luminosities of the hot component, cold component (L_P is the Poynting flux luminosity), and the entire wind, respectively. The parameter σ_0 is defined as

$$\sigma_0 \equiv \frac{L_c}{L_h} = \frac{L_P}{\eta\dot{M}c^2}. \quad (2)$$

For a variable central engine, all the parameters are a function of t . For simplicity, we do not introduce this t -dependence, but focus on the R -dependence of all the parameters.

After escaping from the central engine, the jet undergoes thermal acceleration and magnetic acceleration and gains bulk Lorentz factor. At any radius R , the flow can be categorized by a parameter

$$\mu(R) = \Gamma(R)\Theta(R)(1 + \sigma(R)), \quad (3)$$

where Γ is the bulk Lorentz factor, Θ is the total co-moving energy per baryon ($\Theta - 1$ is the thermal energy), and σ is the ratio between comoving cold (magnetic) and hot (matter) energy densities. Considering a completely cold magnetized outflow, i.e. $\eta = 1$, $\Theta = 1$, and assuming no magnetic dissipation along the way, one would have

$$\mu_0 = 1 + \sigma_0 = \mu = \Gamma(1 + \sigma) = \text{const.} \quad (4)$$

In reality, thermal energy is inevitable, especially when the magnetic energy is dissipated. About half of the dissipated energy is trapped in the system as thermal energy (the other half used to accelerate the flow). As a result, μ would decrease from the original μ_0 when photons escape from the system (e.g. at the photosphere and other dissipation radii above the photosphere). In some models (e.g. ICMART¹⁵), magnetic dissipation proceeds in a run-away manner, so that σ and μ can drop quickly around a certain radius R , and copious photons are released from the system to power the prompt emission.

A thermally driven fireball has a simple Γ -evolution history:^{56–58} Initially the Lorentz factor Γ increases linearly with R until reaching the maximum Lorentz factor essentially defined by central engine baryon loading. The Lorentz factor then “coasts” to the maximum value, reduces at the internal shocks (due to loss of radiation energy), and finally decreases smoothly as a power law beyond the deceleration radius.

A magnetically-driven jet undergoes a more complicated evolution history:^{59–62} For a magnetically dominated jet with initial magnetization σ_0 ($\eta = 1$), the jet would first undergo a rapid acceleration until reaching $R = R_0$ where $\Gamma(R_0) = \sigma_0^{1/3}$ and $\sigma(R_0) = \sigma_0^{2/3}$, and then go through a very slow acceleration process. The fastest acceleration proceeds as $\Gamma \propto R^{1/3}$, either via continuous magnetic dissipation¹³ or via an “impulsive acceleration” of a short pulse.⁶² Ideally, one reaches the maximum Lorentz factor $\Gamma = \sigma_0$ at the coasting radius $R_c = R_0\sigma_0^2$. However, the jet may start to decelerate before reaching the coasting radius if σ_0 is large enough so that $R_c > R_{\text{dec}}$. Also magnetic dissipation can reduce the final coasting Γ , since energy is released as prompt emission.

The Γ -evolution of a hybrid system (with both thermal energy and magnetic energy at the central engine) is more complicated, and has not been studied carefully in the literature. Since thermal acceleration proceeds more rapidly, it would be reasonable to assume that the thermal energy gets converted to kinetic energy first, after which additional acceleration proceeds magnetically if σ_0 is large enough.

4. Debate I: is the jet strongly magnetized at R_{GRB} ?

This is effectively to ask: how high is $\sigma(R_{\text{GRB}})$? The two opponents in the debate and their corresponding arguments are summarized as follows:

- Low $\sigma(R_{\text{GRB}})$ (fireball internal shock model; magnetized engine internal shock model, collisional heating photosphere model:^{5, 6, 38, 39, 47, 49}

8 *Zhang*

- The low- σ model is the simplest, and seems to work reasonably well;
 - We know the physics well, and give more robust predictions;
 - Internal shocks and nuclear collisions are naturally expected in a GRB fireball;
 - Even if the central engine is magnetized, one could have fast magnetic acceleration so that σ is brought below unity so that internal shocks can dissipate the kinetic energy.
- Moderate to high $\sigma(R_{\text{GRB}})$ (magnetic heating photosphere model, IC-MART model, reconnection switch model, current instability model:^{11, 13–16}
 - The broad-band spectra of GRB 080916C show a dominant Band-component covering 6-7 orders of magnitude. Assuming this is the internal shock component, the predicted photosphere component outshines the observed emission.^{41, 63} This suggests that the simplest fireball internal shock model does not explain the data at least for this GRB. This would require a magnetized jet model with suppressed photosphere emission.⁴¹ A good candidate is the ICMART model.¹⁵
 - One way to overcome this difficulty is to introduce a magnetized central engine to suppress the photosphere emission, but demands that the magnetic energy is converted to kinetic energy before internal shocks take place. However, various studies suggest that magnetic acceleration is not an efficient process.^{59–62} It is essentially impossible to have $\sigma(R_{\text{ph}}) \gg 1$, while $\sigma(R_{\text{IS}}) \ll 1$.
 - The internal shock model itself suffers a list of difficulties (see e.g.¹⁵ for a summary): low radiative efficiency, fast cooling, too many electrons to interpret E_p , not easy to interpret the $E_p \propto E_{\text{iso}}^{1/2}$ ⁶⁴ and $E_p \propto L_{\text{iso}}^{1/2}$ ⁶⁵ relations. The difficulties can be overcome if the flow is magnetically dominated and dissipation is through the ICMART process.

5. Debate II: Is the jet energy dissipated via shocks or magnetic reconnection?

This question is closely related to Debate I. If indeed one can have $\sigma(R_{\text{IS}}) \ll 1$, then internal shocks would accelerate electrons to the desired energy to power GRB prompt emission. Recent particle-in-cell (PIC) simulations have shown that magnetic relativistic shocks are not good at accelerating electrons.^{66, 67} For an electron plasma, efficient electron acceleration is possible only when $\sigma \lesssim 10^{-3}$ for relativistic shocks.⁶⁷ For mildly relativistic shocks the constraint is less stringent.⁶⁶ In any case, in order to make internal shocks efficient accelerators, one has double constraints: a not-too-high σ and a not-too-strong shock. The latter constraint further limits the already low dissipation efficiency of shocks.

If $\sigma \gtrsim 1$, the particle acceleration mechanism is likely through magnetic reconnection. In this case, internal shocks can help to facilitate rapid reconnection.^{15, 68}

6. Debate III: Is the dominant radiation mechanism quasi-thermal or non-thermal?

This question is related to the origin of the “Band” spectral component observed in most GRBs, which is dominant spectral component of GRB prompt emission. The two leading interpretations invoke completely different radiation mechanisms. One scenario interprets the spectrum as upscattered quasi-thermal emission from the photosphere, with E_p essentially defined by the photosphere temperature. The other scenario interprets the spectrum as non-thermal emission in the optically thin region. The arguments for each of the above two scenarios include the following:

- Quasi-thermal (dissipative photosphere models^{14, 32, 43, 44, 47–49}): This model interprets the Band component as modified thermal emission from the photosphere. The broadening mechanism includes both physical broadening (Compton upscattering of the seed thermal photons) and geometric broadening (the effect of equal-arrival-time volume).^{32, 33, 69} The arguments that have been raised to support this scenario include:
 - The observed E_p distribution among GRBs is narrow, all around MeV range and below. The photosphere temperature is in this range, and does not sensitively depend on luminosity;⁷⁰
 - The “broadness” of the GRB spectra around E_p , which can be described by a Band function, is relatively “narrow” (compared with the synchrotron peak of other objects, such as blazars). So it is likely of a thermal origin.⁷⁰
 - The photosphere model can interpret⁷¹ the Amati relation⁷² and other correlations, including a correlation between Γ and E_{iso} or L_{iso} .^{73–75}
 - The photosphere emission has a high efficiency. It is hard to avoid a bright photosphere.
- Non-thermal (e.g. internal shock model, ICMART model,^{15, 38, 39, 76–78}): This model interprets the Band component as non-thermal emission of electrons, such as synchrotron or synchrotron self-Compton. The arguments in support of this scenario include the following:
 - The observed E_p distribution among GRBs is actually not that narrow. Considering X-ray flashes (the softer GRBs), E_p can distribute from above MeV to the keV range. More importantly, E_p can evolve rapidly within a same GRB. One can define a “death line” in the $L - E_p$ domain for the dissipative photosphere model that interprets E_p as the temperature of the outflow.⁷⁹ GRB 110721A shows a very high $E_p \sim 15$ MeV early on,²⁴ which is well above the “death line”.⁷⁹ This rules out the thermal origin of E_p at least for this burst (see also⁸⁰). Since the Band function parameters are typical among other GRBs, this would suggest that the Band component in most other GRBs may be also of a non-thermal (e.g. synchrotron) origin.

- Due to a small emission radius, the GRB spectrum predicted in the photosphere model cannot extend to above GeV (due to photon-photon pair production opacity). In some GRBs (e.g. GRB 080916C), the Band component extends to much higher energies.^{20,21} One counter-argument would be that the GeV emission is of an external shock origin.^{81–83} However, it is now clear that the GeV afterglow only sets in after the end of prompt emission,^{21,84–86} and during the prompt emission phase, the GeV emission tracks the variability in the sub MeV regime and should have an internal origin.
- A major difficulty of the photosphere model is that it predicts too hard a low-energy spectrum (with $\alpha \sim +0.4$ ^{47,87}) to match the observed $\alpha = -1$ spectrum. Several efforts to soften the spectrum has been made. 1. Synchrotron radiation is introduced to contribute to emission below E_p . However, the predicted spectrum⁸⁸ does not have the correct shape to interpret the data. In particular, for a softer low energy spectrum, the high energy spectrum is also softened, a behavior not observed from the data. 2. If the high-latitude emission dominates the spectrum, due to the geometric broadening effect one can get $\alpha = -1$.⁸⁹ However, during the prompt emission phase, new materials are continuously ejected, whose emission outshines the high-latitude contribution. The predicted spectrum is still too hard to interpret the data during most of the prompt emission phase. 3. By introducing a special form of angular structured of the jet, one can reproduce $\alpha = -1$.⁶⁹ The special form of the structured jet requires that the luminosity keeps constant in a wide range of angle, while the bulk Lorentz factor drops with angle as a power law. Such a jet structure is most helpful to enhance the high-latitude emission, since a low Γ from the wing allows a wide Γ^{-1} cone to contribute to the on-axis observer. The high-luminosity in the wing (high latitude) then significantly contributes to the observed emission and therefore softens the spectrum. It is however not known how typical such a jet structure is. If both luminosity and Lorentz factor have an angular structure, the photosphere spectrum would then not so different from the uniform jet case, which predicts a harder spectrum.
- The dissipative photosphere models require some tuning of parameters. For example, the magnetic dissipation model requires $\sigma(R_{\text{ph}})$ to be around unity to assure a high radiation efficiency; and the requirement of thermalization poses stringent constraints on the value of Lorentz factor.⁹⁰
- Three independent clues (GeV extension, X-ray tail, and optical association) all point towards a large emission radius R_{GRB} for GRBs.^{15,41,91–93} Although for each argument one has to make the assumption that the sub-MeV emission comes from the same region

as the emission from the other wavelength, when combining all three criteria, it is rather unlikely that only sub-MeV emission comes from the photosphere while emission from other three bands are all from a larger radius.

- Synchrotron models also predict $E_p \propto L^{1/2}$ given that the emission radius R_{GRB} is not very different from burst to burst.⁵³ This may be satisfied for the ICMART model.¹⁵ Other correlations^{73,75,94} can be interpreted with a high- σ central engine model⁵⁴ that invokes the Blandford-Znajek mechanism.⁹⁵
- Very rapid hard-to-soft E_p evolution during the rising phase of the leading GRB pulse^{27,28} could be a big challenge to the photosphere model, but can be interpreted within the framework of synchrotron radiation model.^{15,96}
- In several GRBs a quasi-thermal component is found in superposition with the Band component,^{23,24,97,98} whose temporal evolution is consistent with the photosphere origin.⁹⁹ If this component is of the photosphere origin, then the main Band component must be another component. Since the Band component extends to below the quasi-thermal component, it must not be self-absorbed in the emission region, which means $R_{\text{Band}} \gg R_{\text{ph}}$, i.e. the Band component comes from an optically-thin region far above the photosphere.

7. A breakthrough: fast cooling synchrotron radiation in a decaying magnetic field as the origin of the Band spectral component

Two leading non-thermal radiation mechanisms to interpret GRB prompt emission are synchrotron radiation^{76–78} and synchrotron self-Compton (SSC). The SSC mechanism was particularly suggested to interpret the prompt optical emission of the “naked-eye” GRB 080319B, whose flux significantly exceeds the low-energy extrapolation of the gamma-ray emission.^{100,101} Further studies suggest that this mechanism is disfavored due the following arguments: 1. A dominant SSC component usually predicts an even more dominant 2nd-order SSC component, which greatly adds to the total energy budget of GRBs;^{102,103} 2. This mechanism predicts a strong optical flash. However, observations show that the case of GRB 080319B is rare. Most prompt optical flux is consistent with or below the low-energy extension of gamma-rays;¹⁰⁴ 3. The gamma-ray lightcurve of GRB 080319B is much more variable than the optical lightcurve. Simulations suggest that the SSC and synchrotron lightcurves show similar degree of variability.¹⁰⁵ Besides these criticisms, in general, the SSC mechanism predicts a broader E_p distribution than the synchrotron mechanism due to its sensitive dependence on the electron Lorentz factor γ_e (4th power as compared with 2nd power for the synchrotron mechanism).⁵³

The synchrotron mechanism is known to power non-thermal emission of many

other astrophysical phenomena (e.g. blazars, micro-quasars, supernova remnants, pulsar-wind nebulae). Within the GRB context, the main criticism has been the fast-cooling problem. Since the magnetic field strength is strong in the GRB prompt emission region, electrons lose energy in a time scale much shorter than the dynamical time scale. Traditionally, it was believed that the spectral index below the injection energy due to fast cooling gives a photon index -1.5 , too soft to account for the typical value $\alpha \sim -1$.¹⁰ This has been regarded as a main criticism against the synchrotron mechanism.¹⁰⁶

Recently, a breakthrough was made in modeling synchrotron radiation in GRBs. By introducing a decrease of magnetic field with radius (e.g. due to flux conservation in a conical jet, probably with additional magnetic dissipation), a natural physical ingredient previously ignored in modeling synchrotron cooling, Uhm & Zhang⁹⁶ found that a low-energy spectrum of the fast-cooling synchrotron spectrum is typically harder than -1.5 . By varying model parameters (e.g. the decay index b and the magnetic field normalization B_0 at radius $r_0 = 10^{15}$ cm from the central engine, convention $B(r) = B_0(r/r_0)^{-b}$), one can reproduce a range of α centered around $\alpha \sim -1$, with a distribution from $\alpha \sim -1.5$ to $\alpha > -0.8$. More interestingly, within the typical bandpass of GRB detectors, the synchrotron model spectrum is close to the phenomenological Band function (Fig.1). As a result, we suggest that fast-cooling synchrotron is likely the dominant mechanism that shapes the “Band” component of the observed GRB spectra.

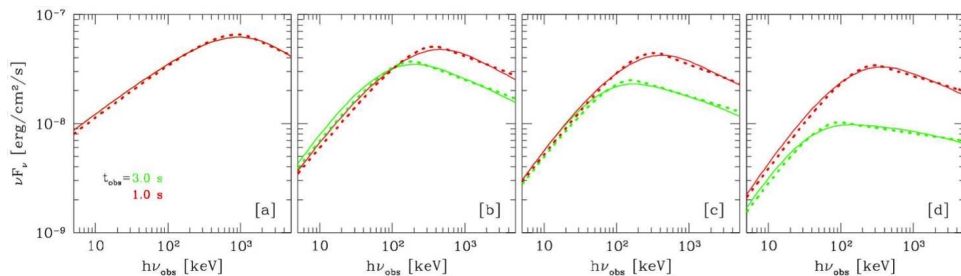


Fig. 1. The model spectra (solid lines) of fast-cooling synchrotron spectrum with a decreasing magnetic field in the emission region, as is naturally expected in the GRB environment. The Band function fits (dotted lines) are over-plotted for comparison. One can see that the fast-cooling synchrotron spectra can mimic the Band function and may provide a reasonable fit to the GRB spectral data. From Uhm & Zhang (2014).⁹⁶

8. GeV emission

Fermi LAT detected emission in the GeV range from a sample of bright GRBs. Two important features of the GeV emission is that some of them have a delayed onset and the emission typically decays as a power law.^{20, 21, 107} This led to the suggestion that the GeV emission is from the external shock.^{81–83} Further studies suggest that

the external shock interpretation applies to phase when the MeV prompt emission is over. During the prompt emission phase, the GeV emission should still have an internal origin.^{84–86}

Several suggestions have been proposed to interpret the delayed onset, e.g. delayed onset of the hadronic component^{108,109} and delayed onset of IC scattering off the cocoon photons.¹¹⁰ On the other hand, the data can be understood in terms of gradual decrease of pair-production opacity,²¹ which may be achieved in a scenario invoking slow acceleration of a magnetized jet.^{51,111}

A hadronic origin of prompt emission has been discussed in the literature.^{109,112} In order to have a dominant hadronic emission component, the proton-to-electron energy ratio has to be large,¹¹³ which greatly increases the energy budget of the bursts. Such a high proton fraction is already constrained by the non-detection of neutrinos from GRBs by IceCube.^{114–117}

9. Putting pieces together

Combining insights gained from multi-wavelength data and theoretical modeling, one may draw the following global picture regarding the origin of GRB prompt emission:

- The Band spectral component originates from an optically thin region with a non-thermal emission mechanism, very likely synchrotron radiation. Fast cooling synchrotron radiation in a decreasing magnetic field gives a simple picture to interpret the Band component, including its typical -1 low energy photon index.⁹⁶ Alternatively, one may introduce slow cooling¹¹⁸ or slow heating due to magnetic turbulence^{15,119} to achieve the right low-energy spectral index.
- The photosphere component has been observed: it can dominate the spectrum in rare cases such as GRB 090902B,^{21,22} but mostly show up as a superposed bump in the low-energy wing of the Band component,^{23,24} or is essentially suppressed (e.g. in GRB 080916C^{20,21,41}).
- The diverse spectral behavior of GRB prompt emission may be related to different σ_0 values at the central engine.⁷⁹ If σ_0 is small enough, one can have a dominant photosphere spectrum as observed in GRB 090902B.^{21,22} If σ_0 is moderately high, the photosphere emission is not completely suppressed, and can have contribution to the observed spectra along with the non-thermal emission from the optically thin region. This applies to the cases such as GRB 100724B²³ and GRB 110721A.²⁴ Finally, if σ_0 is high enough, the photosphere emission is greatly suppressed, and the observed spectrum is dominated by the non-thermal Band component arising from the magnetic dissipation (e.g. ICMART) region.

10. Other clues, future prospects

So far the observational clues are limited to the spectra and lightcurves of GRB prompt emission. Other observational clues can help to further test and constrain the models.

Photon polarization is essential to diagnose jet composition, geometric configuration, and radiation mechanism of GRB jets.¹²⁰ Recently, $> 3\sigma$ polarized gamma-ray signals have been detected in 3 bright GRBs.^{29,30} The degree of polarization is typically very high (several tens of percent). This immediately disfavors the internal shock model that invokes random magnetic fields in the shocked region (due to plasma instabilities) and the non-structured low- σ photosphere models. Models invoking dissipation of ordered magnetic fields, e.g.,^{11,15,16} are favored. A structured jet photosphere model may also produce polarized photons via Compton scattering, but the polarization degree would have a different energy-dependence from the synchrotron model in ordered magnetic fields. A high-sensitivity gamma-ray polarimeter with a wide band-pass to detect energy-dependent polarization signals is essential to constrain these models.

The IceCube Collaboration has placed a more and more stringent high-energy neutrino flux from GRBs.^{114,115} The upper limit starts to challenge the conventional internal shock model.¹¹⁶ A model-dependent study of the GRB neutrino models¹¹⁷ suggests that the neutrino signal would be stronger in the photosphere models than the internal shock model given a same cosmic-ray-to-gamma-ray flux ratio (see also¹²¹). If neutrinos are still not detected from GRBs in the next several years, then the dissipative photosphere models that invoke proton acceleration would be further constrained. Models invoking magnetic dissipation at a large radius¹⁵ are well consistent with the neutrino flux upper limit constraint, and would be supported if neutrinos continue not to be detected to accompany GRBs in the future.

I acknowledge recent stimulative collaborations with Z. L. Uhm, B.-B. Zhang, P. Kumar, A. Pe'er, H. Yan, W. Deng, L. Resmi on the subject of GRB prompt emission. I also thank interesting discussion with the following people on the subject: K. Asano, A. Beloborodov, Z.-G. Dai, F. Daigne, Y.-Z. Fan, H. Gao, D. Giannios, K. Ioka, S. Kobayashi, D. Lazzati, Z. Li, E.-W. Liang, P. Mészáros, R. Mochkovitch, K. Murase, S. Razzaque, F. Ryde, X.-Y. Wang, and X.-F. Wu. This work is supported by NSF AST-0908362.

References

1. B. Zhang, *Comptes Rendus Physique* **12** (April 2011) 206.
2. B. Paczyński, *ApJ* **308** (September 1986) L43.
3. J. Goodman, *ApJ* **308** (September 1986) L47.
4. A. Shemi and T. Piran, *ApJ* **365** (December 1990) L55.
5. P. Mészáros and M. J. Rees, *ApJ* **530** (February 2000) 292.
6. M. J. Rees and P. Mészáros, *ApJ* **430** (August 1994) L93.
7. M. J. Rees and P. Mészáros, *MNRAS* **258** (September 1992) 41P.

8. P. Mészáros and M. J. Rees, *ApJ* **405** (March 1993) 278.
9. P. Mészáros and M. J. Rees, *ApJ* **476** (February 1997) 232.
10. R. Sari, T. Piran and R. Narayan, *ApJ* **497** (April 1998) L17+.
11. M. Lyutikov and R. Blandford, *ArXiv Astrophysics e-prints* (December 2003).
12. H. C. Spruit, F. Daigne and G. Drenkhahn, *A&A* **369** (April 2001) 694.
13. G. Drenkhahn and H. C. Spruit, *A&A* **391** (September 2002) 1141.
14. D. Giannios, *A&A* **480** (March 2008) 305.
15. B. Zhang and H. Yan, *ApJ* **726** (January 2011) 90.
16. J. C. McKinney and D. A. Uzdensky, *MNRAS* **419** (January 2012) 573.
17. G. J. Fishman and C. A. Meegan, *Annual Review of Astronomy and Astrophysics* **33** (1995) 415.
18. H. Gao, B.-B. Zhang and B. Zhang, *ApJ* **748** (April 2012) 134.
19. D. Band, J. Matteson, L. Ford, B. Schaefer, D. Palmer, B. Teegarden, T. Cline, M. Briggs, W. Paciesas, G. Pendleton, G. Fishman, C. Kouveliotou, C. Meegan, R. Wilson and P. Lestrade, *ApJ* **413** (August 1993) 281.
20. A. A. Abdo, M. Ackermann, M. Arimoto, K. Asano, W. B. Atwood, M. Axelsson, L. Baldini, J. Ballet, D. L. Band, G. Barbiellini and et al., *Science* **323** (March 2009) 1688.
21. B.-B. Zhang, B. Zhang, E.-W. Liang, Y.-Z. Fan, X.-F. Wu, A. Pe'er, A. Maxham, H. Gao and Y.-M. Dong, *ApJ* **730** (April 2011) 141.
22. F. Ryde, M. Axelsson, B. B. Zhang, S. McGlynn, A. Pe'er, C. Lundman, S. Larsson, M. Battelino, B. Zhang, E. Bissaldi, J. Bregeon, M. S. Briggs, J. Chiang, F. de Palma, S. Guiriec, J. Larsson, F. Longo, S. McBreen, N. Omodei, V. Petrosian, R. Preece and A. J. van der Horst, *ApJ* **709** (February 2010) L172.
23. S. Guiriec, V. Connaughton, M. S. Briggs, M. Burgess, F. Ryde, F. Daigne, P. Mészáros, A. Goldstein, J. McEnery, N. Omodei, P. N. Bhat, E. Bissaldi, A. Camero-Arranz, V. Chaplin, R. Diehl, G. Fishman, S. Foley, M. Gibby, M. M. Giles, J. Greiner, D. Gruber, A. von Kienlin, M. Kippen, C. Kouveliotou, S. McBreen, C. A. Meegan, W. Paciesas, R. Preece, A. Rau, D. Tierney, A. J. van der Horst and C. Wilson-Hodge, *ApJ* **727** (February 2011) L33.
24. M. Axelsson, L. Baldini, G. Barbiellini, M. G. Baring, R. Bellazzini, J. Bregeon, M. Brigida, P. Bruel, R. Buehler, G. A. Caliandro and et al., *ApJ* **757** (October 2012) L31.
25. M. Ackermann, M. Ajello, K. Asano, M. Axelsson, L. Baldini, J. Ballet, G. Barbiellini, M. G. Baring, D. Bastieri and K. e. a. Bechtol, *ApJ* **729** (March 2011) 114.
26. S. Campana, V. Mangano, A. J. Blustin, P. Brown, D. N. Burrows, G. Chincarini, J. R. Cummings, G. Cusumano, M. Della Valle, D. Malesani, P. Mészáros, J. A. Nousek, M. Page, T. Sakamoto, E. Waxman, B. Zhang, Z. G. Dai, N. Gehrels, S. Immler, F. E. Marshall, K. O. Mason, A. Moretti, P. T. O'Brien, J. P. Osborne, K. L. Page, P. Romano, P. W. A. Roming, G. Tagliaferri, L. R. Cominsky, P. Giommi, O. Godet, J. A. Kennea, H. Krimm, L. Angelini, S. D. Barthelmy, P. T. Boyd, D. M. Palmer, A. A. Wells and N. E. White, *Nature* **442** (August 2006) 1008.
27. R.-J. Lu, S.-J. Hou and E.-W. Liang, *ApJ* **720** (September 2010) 1146.
28. R.-J. Lu, J.-J. Wei, E.-W. Liang, B.-B. Zhang, H.-J. Lü, L.-Z. Lü, W.-H. Lei and B. Zhang, *ApJ* **756** (September 2012) 112.
29. D. Yonetoku, T. Murakami, S. Gunji, T. Mihara, K. Toma, T. Sakashita, Y. Morihara, T. Takahashi, N. Toukairin, H. Fujimoto, Y. Kodama, S. Kubo and IKAROS Demonstration Team, *ApJ* **743** (December 2011) L30.
30. D. Yonetoku, T. Murakami, S. Gunji, T. Mihara, K. Toma, Y. Morihara, T. Takahashi, Y. Wakashima, H. Yonemochi, T. Sakashita, N. Toukairin, H. Fujimoto and

- Y. Kodama, *ApJ* **758** (October 2012) L1.
31. B. Zhang, Y. Z. Fan, J. Dyks, S. Kobayashi, P. Mészáros, D. N. Burrows, J. A. Nousek and N. Gehrels, *ApJ* **642** (May 2006) 354.
 32. A. Pe'er, *ApJ* **682** (July 2008) 463.
 33. A. M. Beloborodov, *ApJ* **737** (August 2011) 68.
 34. R. Narayan and P. Kumar, *MNRAS* **394** (March 2009) L117.
 35. P. Kumar and R. Narayan, *MNRAS* **395** (May 2009) 472.
 36. S. Kobayashi, T. Piran and R. Sari, *ApJ* **490** (November 1997) 92.
 37. F. Daigne and R. Mochkovitch, *MNRAS* **296** (May 1998) 275.
 38. Ž. Bošnjak, F. Daigne and G. Dubus, *A&A* **498** (May 2009) 677.
 39. F. Daigne, Ž. Bošnjak and G. Dubus, *A&A* **526** (February 2011) A110.
 40. F. Daigne and R. Mochkovitch, *MNRAS* **336** (November 2002) 1271.
 41. B. Zhang and A. Pe'er, *ApJ* **700** (August 2009) L65.
 42. R. Hascoët, F. Daigne and R. Mochkovitch, *A&A* **551** (March 2013) A124.
 43. C. Thompson, *MNRAS* **270** (October 1994) 480.
 44. M. J. Rees and P. Mészáros, *ApJ* **628** (August 2005) 847.
 45. C. Thompson, *ApJ* **651** (November 2006) 333.
 46. G. Ghisellini, A. Celotti, G. Ghirlanda, C. Firmani and L. Nava, *MNRAS* **382** (November 2007) L72.
 47. A. M. Beloborodov, *MNRAS* **407** (September 2010) 1033.
 48. D. Lazzati and M. C. Begelman, *ApJ* **725** (December 2010) 1137.
 49. K. Ioka, *Progress of Theoretical Physics* **124** (October 2010) 667.
 50. D. Lazzati, B. J. Morsony and M. C. Begelman, *ApJ* **732** (May 2011) 34.
 51. P. Mészáros and M. J. Rees, *ApJ* **733** (June 2011) L40.
 52. P. Veres and P. Mészáros, *ApJ* **755** (August 2012) 12.
 53. B. Zhang and P. Mészáros, *ApJ* **581** (December 2002) 1236.
 54. W.-H. Lei, B. Zhang and E.-W. Liang, *ApJ* **765** (March 2013) 125.
 55. B. D. Metzger, D. Giannios, T. A. Thompson, N. Bucciantini and E. Quataert, *MNRAS* **413** (May 2011) 2031.
 56. P. Mészáros, P. Laguna and M. J. Rees, *ApJ* **415** (September 1993) 181.
 57. T. Piran, A. Shemi and R. Narayan, *MNRAS* **263** (August 1993) 861.
 58. S. Kobayashi, T. Piran and R. Sari, *ApJ* **513** (March 1999) 669.
 59. S. S. Komissarov, N. Vlahakis, A. Königl and M. V. Barkov, *MNRAS* **394** (April 2009) 1182.
 60. Y. E. Lyubarsky, *MNRAS* **402** (February 2010) 353.
 61. A. Tchekhovskoy, R. Narayan and J. C. McKinney, *New Astron.* **15** (November 2010) 749.
 62. J. Granot, S. S. Komissarov and A. Spitkovsky, *MNRAS* **411** (February 2011) 1323.
 63. Y. Fan, *MNRAS* **403** (March 2010) 483.
 64. L. Amati, F. Frontera, M. Tavani, J. J. M. in't Zand, A. Antonelli, E. Costa, M. Feroci, C. Guidorzi, J. Heise, N. Masetti, E. Montanari, L. Nicastro, E. Palazzi, E. Pian, L. Piro and P. Soffitta, *A&A* **390** (July 2002) 81.
 65. D. Yonetoku, T. Murakami, T. Nakamura, R. Yamazaki, A. K. Inoue and K. Ioka, *ApJ* **609** (July 2004) 935.
 66. L. Sironi and A. Spitkovsky, *ApJ* **698** (June 2009) 1523.
 67. L. Sironi and A. Spitkovsky, *ApJ* **726** (January 2011) 75.
 68. L. Sironi and A. Spitkovsky, *ApJ* **741** (November 2011) 39.
 69. C. Lundman, A. Pe'er and F. Ryde, *MNRAS* **428** (January 2013) 2430.
 70. A. M. Beloborodov, *ApJ* **764** (February 2013) 157.
 71. Y.-Z. Fan, D.-M. Wei, F.-W. Zhang and B.-B. Zhang, *ApJ* **755** (August 2012) L6.

72. C. Thompson, P. Mészáros and M. J. Rees, *ApJ* **666** (September 2007) 1012.
73. E.-W. Liang, S.-X. Yi, J. Zhang, H.-J. Lü, B.-B. Zhang and B. Zhang, *ApJ* **725** (December 2010) 2209.
74. G. Ghirlanda, L. Nava, G. Ghisellini, A. Celotti, D. Burlon, S. Covino and A. Melandri, *MNRAS* **420** (February 2012) 483.
75. J. Lü, Y.-C. Zou, W.-H. Lei, B. Zhang, Q. Wu, D.-X. Wang, E.-W. Liang and H.-J. Lü, *ApJ* **751** (May 2012) 49.
76. P. Mészáros, M. J. Rees and H. Papathanassiou, *ApJ* **432** (September 1994) 181.
77. M. Tavani, *ApJ* **466** (August 1996) 768.
78. N. M. Lloyd and V. Petrosian, *ApJ* **543** (November 2000) 722.
79. B. Zhang, R.-J. Lu, E.-W. Liang and X.-F. Wu, *ApJ* **758** (October 2012) L34.
80. P. Veres, B.-B. Zhang and P. Mészáros, *ApJ* **761** (December 2012) L18.
81. P. Kumar and R. Barniol Duran, *MNRAS* **400** (November 2009) L75.
82. P. Kumar and R. Barniol Duran, *MNRAS* **409** (November 2010) 226.
83. G. Ghisellini, G. Ghirlanda, L. Nava and A. Celotti, *MNRAS* **403** (April 2010) 926.
84. A. Maxham, B.-B. Zhang and B. Zhang, *MNRAS* **415** (July 2011) 77.
85. H.-N. He, X.-F. Wu, K. Toma, X.-Y. Wang and P. Mészáros, *ApJ* **733** (May 2011) 22.
86. R.-Y. Liu and X.-Y. Wang, *ApJ* **730** (March 2011) 1.
87. Deng, W. and Zhang, B. *ApJ*, in press, arXiv:1402.5364 (2014)
88. I. Vurm, A. M. Beloborodov and J. Poutanen, *ApJ* **738** (September 2011) 77.
89. A. Pe'er and F. Ryde, *ApJ* **732** (May 2011) 49.
90. I. Vurm, Y. Lyubarsky and T. Piran, *ApJ* **764** (February 2013) 143.
91. P. Kumar, E. McMahon, A. Panaitescu, R. Willingale, P. O'Brien, D. Burrows, J. Cummings, N. Gehrels, S. Holland, S. B. Pandey, D. vanden Berk and S. Zane, *MNRAS* **376** (March 2007) L57.
92. N. Gupta and B. Zhang, *MNRAS* **384** (February 2008) L11.
93. R. Hascoët, F. Daigne and R. Mochkovitch, *A&A* **542** (June 2012) L29.
94. G. Ghirlanda, G. Ghisellini, L. Nava and D. Burlon, *MNRAS* **410** (January 2011) L47.
95. R. D. Blandford and R. L. Znajek, *MNRAS* **179** (May 1977) 433.
96. Z. L. Uhm and B. Zhang, *Nature Physics*, in press, arXiv:1303.2704 (2014)
97. F. Ryde, *ApJ* **625** (June 2005) L95.
98. S. Guiriec, F. Daigne, R. Hascoët, G. Vianello, F. Ryde, R. Mochkovitch, C. Kouveliotou, S. Xiong, P. N. Bhat, S. Foley, D. Gruber, J. M. Burgess, S. McGlynn, J. McEnery and N. Gehrels, *ApJ* **770** (June 2013) 32.
99. F. Ryde and A. Pe'er, *ApJ* **702** (September 2009) 1211.
100. J. L. Racusin, S. V. Karpov, M. Sokolowski, J. Granot, X. F. Wu, V. Pal'Shin, S. Covino, A. J. van der Horst, S. R. Oates, P. Schady, R. J. Smith, J. Cummings, R. L. C. Starling, L. W. Piotrowski, B. Zhang, P. A. Evans, S. T. Holland, K. Malek, M. T. Page, L. Vetere, R. Margutti, C. Guidorzi, A. P. Kamble, P. A. Curran, A. Beardmore, C. Kouveliotou, L. Mankiewicz, A. Melandri, P. T. O'Brien, K. L. Page, T. Piran, N. R. Tanvir, G. Wrochna, R. L. Aptekar, S. Barthelmy, C. Bartolini, G. M. Beskin, S. Bondar, M. Bremer, S. Campana, A. Castro-Tirado, A. Cucchiara, M. Cwiok, P. D'Avanzo, V. D'Elia, M. D. Valle, A. de Ugarte Postigo, W. Dominik, A. Falcone, F. Fiore, D. B. Fox, D. D. Frederiks, A. S. Fruchter, D. Fugazza, M. A. Garrett, N. Gehrels, S. Golenetskii, A. Gomboc, J. Gorosabel, G. Greco, A. Guarneri, S. Immler, M. Jelinek, G. Kasprovicz, V. La Parola, A. J. Levan, V. Mangano, E. P. Mazets, E. Molinari, A. Moretti, K. Nawrocki, P. P. Oleynik, J. P. Osborne, C. Pagani, S. B. Pandey, Z. Paragi, M. Perri, A. Piccioni, E. Ramirez-Ruiz, P. W. A.

- Roming, I. A. Steele, R. G. Strom, V. Testa, G. Tosti, M. V. Ulanov, K. Wiersema, R. A. M. J. Wijers, J. M. Winters, A. F. Zarnecki, F. Zerbi, P. Mészáros, G. Chincarini and D. N. Burrows, *Nature* **455** (September 2008) 183.
101. P. Kumar and A. Panaitescu, *MNRAS* **391** (November 2008) L19.
 102. E. V. Derishev, V. V. Kocharovskiy and V. V. Kocharovskiy, *A&A* **372** (June 2001) 1071.
 103. T. Piran, R. Sari and Y.-C. Zou, *MNRAS* **393** (March 2009) 1107.
 104. R. Shen and B. Zhang, *MNRAS* **398** (October 2009) 1936.
 105. L. Resmi and B. Zhang, *MNRAS* **426** (October 2012) 1385.
 106. G. Ghisellini, A. Celotti and D. Lazzati, *MNRAS* **313** (March 2000) L1.
 107. A. A. Abdo, M. Ackermann, M. Ajello, K. Asano, W. B. Atwood, M. Axelsson, L. Baldini, J. Ballet, G. Barbiellini, M. G. Baring and et al., *Nature* **462** (November 2009) 331.
 108. S. Razzaque, C. D. Dermer and J. D. Finke, *The Open Astronomy Journal* **3** (August 2010) 150.
 109. K. Asano and P. Mészáros, *ApJ* **757** (October 2012) 115.
 110. K. Toma, X. Wu and P. Mészáros, *ApJ* **707** (December 2009) 1404.
 111. Ž. Bošnjak and P. Kumar, *MNRAS* **421** (March 2012) L39.
 112. K. Asano, S. Guiriec and P. Mészáros, *ApJ* **705** (November 2009) L191.
 113. N. Gupta and B. Zhang, *MNRAS* **380** (September 2007) 78.
 114. R. Abbasi, Y. Abdou, T. Abu-Zayyad, J. Adams, J. A. Aguilar, M. Ahlers, K. Andeen, J. Auffenberg, X. Bai, M. Baker and et al., *Physical Review Letters* **106** (April 2011) 141101.
 115. R. Abbasi, Y. Abdou, T. Abu-Zayyad, M. Ackermann, J. Adams, J. A. Aguilar, M. Ahlers, D. Altmann, K. Andeen, J. Auffenberg and et al., *Nature* **484** (April 2012) 351.
 116. H.-N. He, R.-Y. Liu, X.-Y. Wang, S. Nagataki, K. Murase and Z.-G. Dai, *ApJ* **752** (June 2012) 29.
 117. B. Zhang and P. Kumar, *Physical Review Letters* **110** (March 2013) 121101.
 118. A. Pe’er and B. Zhang, *ApJ* **653** (December 2006) 454.
 119. K. Asano and T. Terasawa, *ApJ* **705** (November 2009) 1714.
 120. K. Toma, T. Sakamoto, B. Zhang, J. E. Hill, M. L. McConnell, P. F. Bloser, R. Yamazaki, K. Ioka and T. Nakamura, *ApJ* **698** (June 2009) 1042.
 121. S. Gao, K. Asano and P. Mészáros, *JCAP* **11** (November 2012) 58.